Article

Not peer-reviewed version

Modeling the *D. citri*-HLB Pathosystem

Sandra L. Franco-García * , Fabio A. Milner , Lilian S. Sepúlveda Salcedo

Posted Date: 1 January 2026

doi: 10.20944/preprints202601.0045.v1

Keywords: dynamical system; agricultural pest; mathematical model; Huanglongbing (HLB); *Diaphorina citri; Citrus x latifolia*; *Tamarixia radiata*; integrated pest management (IPM)

 doi:10.20944/preprints202601.0045.v1

Article

Modeling the *D. citri*-HLB Pathosystem

Sandra L. Franco-Garcia [1,2,*], Fabio A. Milner [3] and Lilian S. Sepúlveda Salcedo [4]

[1] Insterinstitutional Doctorate in Enviromental Science, Universidad del Cauca, Popayán, Colombia
[2] Universidad del Valle, Cali, Colombia
[3] Arizona State University, Tempe, AZ, USA
[4] Facultad de Ingenirías y Ciencias Básicas, Universidad Autónoma de Occidente, Cali, Colombia
* Correspondence: sandrafranco@unicauca.edu.co; Tel.: +57-3173242722

Abstract

Vector-borne plant diseases represent a complex phytosanitary challenge. Mathematical models serve as a key tool for analyzing integrated management strategies, enabling more effective control of these pests. A dynamical system is presented to model the infection of Tahiti lime (*Citrus x latifolia*) with the bacterium *Candidatus* Liberibacter asiaticus (CLas), transmitted mainly by infected adults of the psyllid *D. citri*, which causes the *citrus greening* —Huanglongbing (HLB). The proposed model is based on the *D. citri*-HLB pathosystem, basic interactions between bacteria, vector psyllid hosts, trees and a vector parasitoid wasp. It consists of nine ordinary differential equations that model the rates of change of the numbers of infected and uninfected vector nymphs and adult females, of infected and uninfected trees of high and low productivity, and of the parasitoid *Tamarixia radiata*, recommended for the biological control of *D. citri*. The parameters of the model are identified from extant literature or otherwise estimated, in both cases being adjusted to Colombian conditions. A mathematical analysis of a simplified model is carried out, and simulations are conducted to demonstrate the effect of different types of control measures.

Keywords: dynamical system; agricultural pest; mathematical model; Huanglongbing (HLB); *Diaphorina citri*; *Citrus x latifolia*; *Tamarixia radiata*; integrated pest management (IPM)

1. Introduction

Citrus Huanglongbing (HLB) represents one of the most devastating threats to citrus production worldwide. This disease is caused by bacteria of the genus *Candidatus* Liberibacter spp. (variants asiaticus, americanus and africanus), the asiaticus strain being the one present in Colombia, where it is transmitted by the psyllid *Diaphorina citri* Kuwayama. It was first detected in the Tolima Department of Colombia in 2008 and it has since become established in at least six departments in the north of the country. HLB causes a variety of symptoms, including foliar discoloration, fruit deformation, and eventual tree decline, drastically reducing citrus crop productivity and quality, rendering fruit inedible, and ultimately destroying trees [1,2].

Globally, inadequate management strategies have caused severe regional economic impacts: annual losses of USD 1 billion in Florida, USA [3], an increase in production costs of USD 153 million in Mexico [4] and a 68% decline in Brazil's fruit production in five years [5]. Therefore, it is important to reassess production and management strategies. In Colombia, although the disease arrived later, its presence has been confirmed in approximately 20% of the citrus production regions [6].

Control strategies for HLB focus on integrated measures, including the use of resistant or tolerant varieties, cultural management such as removal of infected trees, chemical control of the vector, orchard management practices to reduce disease incidence [3], and biological control through parasitoids specific of *D. citri*, such as the wasp *T. radiata* [7]. These practices not only aim to mitigate the spread of pathogens, but also to maintain the long-term viability of citrus production systems.

 doi:10.20944/preprints202601.0045.v1

We propose a mathematical model to describe the dynamics of the *D. citri*-HLB pathosystem, considering some of the most common control practices. We aim to simulate integrated management strategies and to compare the effectiveness of these control practices —individually or in combination— with the goal of evaluating potential bioeconomic strategies for more effective HLB control in the future. We carry out the analysis of a reduced dynamical system model, including local and global existence and uniqueness of solutions, global preservation of positivity, and the existence and stability of up to three steady states:

- The extinction equilibrium —locally asymptotically stable when the basic reproduction number of *D. citri*, $\mathscr{R}_0^D$, is smaller than 1 (in which case it is the only steady state), and unstable when it is larger than 1;
- an equilibrium with *D. citri* nymphs and adults but no *T. radiata* that exists only when $\mathscr{R}_0^D > 1$; and
- a coexistence equilibrium of vectors and parasitoids.

2. Materials and Methods

In this section, a nonlinear ODE system is described to model the life cycle of the psyllid summarized in just the two compartments that are important for the dynamics of citrus trees infections with HLB. They are *D. citri* adults and stages-3-to-5 nymphs, because later nymphal stages are considered the most efficient at acquiring and replicating the bacterium [8] and additionally these are the only stages that can be parasitized by *T. radiata* [9]. Furthermore, group nymphs in stages 3–5 can be merged into a single compartment because there is no appreciable difference in the interactions of those three stages of nymphs with the citrus trees, with the HLB bacteria, or with the *T. radiata* wasps. Given the demonstrated low bacterial uptake capacity in adult *D. citri* [10], it restricts the infectious *D. citri* adults to psyllids that acquired CLas as nymphs.

In summary, we neglect the egg, nymph-1, and nymph-2 stages of *D. citri* and simplify the model to collapse oviposition, transition from egg to nymph, and the first two moultings, into a single transition from adult to stage-3 nymph.

To keep the model simple, we do not consider the difference between infected and infectious *D. citri*, that is, we do not consider an incubation period.

Consequently, the psyllid population is divided into four compartments, with the following sizes at time $t \geq 0$:

- $N(t)$:= number of *D. citri* stage 3–4–5 nymphs not carrying bacteria CLas (i.e., uninfected nymphs);
- $N_i(t)$:= number of *D. citri* stage 3–4–5 nymphs carrying bacteria CLas (i.e., infected/infectious nymphs);
- $A(t)$:= number of *D. citri* adults that do not transmit the HLB.
- $A_i(t)$:= number of *D. citri* adults that transmit the HLB.

We also divide the citrus tree population into four compartments, with the following sizes at time $t \geq 0$:

- $T_1(t)$:= number of citrus trees with high sprouting and fruit production, and free of HLB
- $T_{1i}(t)$:= number of citrus trees with high sprouting and fruit production, and infected with HLB
- $T_2(t)$:= number of citrus trees with low sprouting and fruit production, and free of HLB.
- $T_{2i}(t)$:= number of citrus trees with low sprouting and fruit production, and infected with HLB

Throughout this paper, we will use the expression *infected trees* to mean citrus trees infected with HLB and, *a fortiori*, also with HLB-infected *D. citri*. However, *uninfected trees* will mean they are free of HLB though not necessarily of *D. citri*. If an uninfected tree has *D. citri* nymphs on its shoots, they must necessarily be HLB-free nymphs. The *T. radiata* population considered consists only of adult females because this is the stage in which they can parasitize *D. citri* nymphs. Thus, the dynamics of the wasp population is modeled with a single compartment, with the following size at time $t \geq 0$:

- $W(t)$:= number of adult female *T. radiata*

 doi:10.20944/preprints202601.0045.v1

We make several assumptions in order to simplify the model while still capturing the essential features of interactions among the various species and also allowing for the different types of interventions that we want to consider:

- The per capita "oviposition" rate of adult *D. citri*, ρ, is actually the product of four factors: their natural per capita egg-laying (=*oviposition*) rate, the probability of survival from egg to nymph-1 stage, the probability of survival from nymph-1 to nymph-2 stage, and the probability of survival from nymph-2 to nymph-3 stage. Hence the quotation marks around 'oviposition'.
- The per capita oviposition rate of adult *D. citri* is the same whether they are healthy or infected; thus the generation of new nymphs does not depend on whether they originate from a healthy or an infected adult.
- Nymphs that hatch on a healthy tree are considered healthy, while those that hatch on an HLB-infected tree are considered infected, regardless of the HLB-infection status of the adult parent. This is justified because, as far as we know, HLB is not transmitted vertically from adult female moths to their offspring to daughter.
- Because oviposition and nymph development take place only on citrus tree shoots, we assume that the availability or scarcity of the latter impacts the natural oviposition rate through a factor that is an increasing function of the total number of shoots of the corresponding infection status, with values between 0 and 1.
- Because *D. citri* nymphs are immobile, they do not have logistic per capita mortality driven by intra-species competition.
- Because the livelihood of adult *D. citri* is intimately tied to the availability of citrus tree shoots to feed on, logistic mortality from intra-species competition is assumed to occur at a rate that decreases with increasing availability of shoots of any infection status.
- Because adult *D. citri* who get infected with HLB from feeding on shoots from an infected tree have too short a life-span to develop a pathogen load high enough to further transmit infection to uninfected trees when feeding on their shoots, we do not consider such feeding as a source of infected adults since we only want the compartment A_i to contain infectious adults and not infected-but-not-infectious.
- Because *T. radiata* deposes its eggs only in *D. citri* nymphs —only one egg per nymph— and this results in the death of the nymph, the per capita *T. radiata*-induced mortality rate of *D. citri* nymphs is assumed to be proportional to the number of *T. radiata* wasps.
- *D. citri* adults are considered infected only if they originate from infected nymphs.
- *D. citri* nymphs may die due to natural causes, to the effect of agrochemical products used for their control, or to parasitism by *T. radiata*.
- *D. citri* adults may die due to natural causes or as a result of agrochemical control.
- We do not include the planting of new trees. Therefore, the total tree population can only decrease.
- Trees are classified into high-fitness —producing a commercially acceptable amount of fruit— and low-fitness —with very low and commercially negligible production.
- Irrespective of their fitness, trees can develop HLB only if an infected *D. citri* adult feeds on them.
- The only way for a high-fitness tree to transition to low fitness is through neglect, irrespective of whether it is healthy or HLB-infected.
- A healthy low-fitness tree can recover and transition to high fitness with proper care.
- An HLB-infected low-fitness tree cannot recover and regain high fitness, because of the disease.
- Irrespective of their fitness, healthy trees produce healthy shoots and HLB-infected trees produce infected shoots.
- HLB-infected trees, whether of high or low fitness, may be eradicated as a control measure.
- *T. radiata* wasps experience natural mortality and may also die from the effect of agrochemicals applied for the control of *D. citri*.

The dynamics of the system is described by the following system of nine ordinary differential equations, four for the psyllid, four for the citrus trees, and one for the parasitoid.

 doi:10.20944/preprints202601.0045.v1

$$\frac{dN}{dt} = \rho(A+A_i)\frac{b}{b+b_i} - \mu_N N - \gamma N - \xi W N - \delta_N(t)N \tag{2.1a}$$

$$\frac{dN_i}{dt} = \rho(A+A_i)\frac{b_i}{b+b_i} - \mu_N N_i - \gamma N_i - \xi W N_i - \delta_N(t)N_i \tag{2.1b}$$

$$\frac{dA}{dt} = \gamma N - \left(\mu_A + \frac{C_A}{b+b_i}(A+A_i)\right)A - \delta_A(t)A \tag{2.1c}$$

$$\frac{dA_i}{dt} = \gamma N_i - \left(\mu_A + \frac{C_A}{b+b_i}(A+A_i)\right)A_i - \delta_A(t)A_i \tag{2.1d}$$

$$\frac{dT_1}{dt} = \tau T_2 - \lambda T_1 - \theta_T \frac{A_i}{\eta + A + A_i}T_1 \tag{2.1e}$$

$$\frac{dT_{1i}}{dt} = \theta_T \frac{A_i}{\eta + A + A_i}T_1 - \lambda_i T_{1i} - \alpha_1 T_{1i} \tag{2.1f}$$

$$\frac{dT_2}{dt} = \lambda T_1 - \mu_{T_2} T_2 - \tau T_2 - \theta_T \frac{A_i}{\eta + A + A_i}T_2 \tag{2.1g}$$

$$\frac{dT_{2i}}{dt} = \lambda_i T_{1i} + \theta_T \frac{A_i}{\eta + A + A_i}T_2 - \mu_{T_{2i}} T_{2i} - \alpha_2 T_{2i} \tag{2.1h}$$

$$\frac{dW}{dt} = \Lambda(t) + \xi\left(\frac{N+N_i}{\nu + N + N_i}\right)W - \mu_W W - \delta_W(t)W \tag{2.1i}$$

where

$$\begin{aligned} b &= m_1 T_1 + m_2 T_2 && = \text{total number of shoots in trees free of HLB,} \\ b_i &= m_{1i} T_{1i} + m_{2i} T_{2i} && = \text{total number of shoots in trees infected with HLB.} \end{aligned} \tag{2.2}$$

It is assumed that the average number of shoots for each of the four types of trees —m_1, m_2, m_{1i}, m_{2i}— stays constant in time. Concerning control measures, assume that agrochemicals affect *D. citri* the same way irrespective of their infection status, but differentially for nymphs and adults. We also assume that agrochemicals induce additional mortality for *T. radiata* as an undesired side effect.

 doi:10.20944/preprints202601.0045.v1

Table 1. Description of parameters of the *D. citri* model.

Symbol	Description
ρ	maximal per capita production rate of *D. citri* 3rd-instar nymphs (per adult)
m_1	average number of shoots per high-sprouting uninfected tree
m_{1i}	average number of shoots per high-sprouting infected tree
m_2	average number of shoots per low-sprouting uninfected tree
m_{2i}	average number of shoots per low-sprouting infected tree
μ_N	natural per capita mortality rate of stages 3–5 nymphs
μ_A	natural per capita mortality rate of adult *D. citri*
μ_{T_2}	per capita mortality rate of low-productivity uninfected trees
$\mu_{T_{2i}}$	per capita mortality rate of low-productivity infected trees
μ_W	per capita mortality rate of *T. radiata*
γ	per capita transition rate of stage 3–5 nymphs to adulthood
ξ	per capita oviposition rate of *T. radiata*
$\delta_N(t)$	per capita mortality rate of *D. citri* nymphs from agrochemicals
$\delta_A(t)$	per capita mortality rate of adult *D. citri* from agrochemicals
$\delta_W(t)$	per capita mortality rate of *T. radiata* from agrochemicals
C_A	intra-specific competition constant in adult *D. citri* mortality per sprout
θ_T	per capita infection rate of trees by adult *D. citri* when all of them are infected
τ	per capita transition rate of low-productivity trees to high productivity
λ	per capita transition rate of uninfected trees from high to low productivity
λ_i	per capita transition rate of infected trees from high to low productivity
α_1	per capita eradication rate of high-productivity trees with HLB
α_2	per capita eradication rate of low-productivity trees with HLB
$\Lambda(t)$	per capita release rate of *T. radiata*
ν	number of nymphs in stages 3–5 resulting in 50% reduction of *T. radiata*
η	fraction of adult *D. citri* to keep tree infection rate continuous at $A = A_i = 0$

3. Results

3.1. Mathematical Analysis of a Reduced Model

Let us denote the total adult *D. citri* population size as $x(t) = A(t) + A_i(t)$, and the total *D. citri* nymph population size as $y(t) = N(t) + N_i(t)$. Then, summing equations (2.1c) with (2.1d) and (2.1a) with (2.1b), we see that *D. citri* adults, *D. citri* nymphs, and *T. radiata* satisfy the following system of ODEs:

$$\frac{dx}{dt} = \gamma y - \left(\mu_A + \delta_A(t) + \frac{C_A}{B}x\right)x, \tag{3.1}$$

$$\frac{dy}{dt} = \rho x - \left(\mu_N + \gamma + \xi W + \delta_N(t)\right)y, \tag{3.2}$$

$$\frac{dW}{dt} = \Lambda(t) + \xi\left(\frac{y}{\nu + y}\right)W - \mu_W W - \delta_W(t)W, \tag{3.3}$$

 doi:10.20944/preprints202601.0045.v1

where $B = B(t) = b(t) + b_i(t)$ is the total number of shoots on the plantation's trees, which we will assume constant for this analysis. We shall also assume that the only control measure used is the parasitoid *T. radiata*, so that $\delta_W \equiv 0$, and that no wasps are released after an initial release that left their population's fate up to having enough nymphs to lay their eggs in, i.e. $\Lambda(t) \equiv 0$.

3.1.1. Well-Posedness

The well-posedness of the reduced system

$$\begin{aligned} \frac{dx}{dt} &= \gamma y - \left(\mu_A + \frac{C_A}{B}x\right)x, \\ \frac{dy}{dt} &= \rho x - (\mu_N + \gamma + \xi W)y, \\ \frac{dW}{dt} &= \xi\left(\frac{y}{\nu + y}\right)W - \mu_W W, \end{aligned} \tag{3.4}$$

follows from the general existence and uniqueness theorem for systems of ODEs. That is,

Theorem 1. *Let $t_0 \in \mathbb{R}$ and $X_0 = (x_0, y_0, W_0)^T \in \mathbb{R}^3$ be arbitrary, with $y_0 \neq -\nu$. Then, there exists $h > 0$ such that the system (3.4) has a unique solution $X(t) = [x(t), y(t), W(t)]^T$ for $t \in (t_0 - h, t_0 + h)$ which satisfies $X(t_0) = X_0$.*

We can also prove that the system also gives ecologically meaningful solutions. That is,

Theorem 2. *For any initial condition $(x_0, y_0, W_0) \in \mathbb{R}^3_+$ (the non-negative cone of $\mathbb{R}^3$), the system (3.4) has a unique, non-negative solution $X(t) = [x(t), y(t), W(t)]^T$ for $t \in [t_0, \infty)$ which satisfies $X(t_0) = X_0$.*

Proof. First note that, for any function $y \in L^1_{\text{loc}}([0, \infty))$ bounded away from $-\nu$, for any $W_0 \geq 0$, and for all $t \geq 0$,

$$W(t) = W_0 \exp\left(\int_0^t \left[\frac{\xi y(s)}{\nu + y(s)} - \mu_W\right] ds\right) \geq 0, \tag{3.5}$$

and $W = 0$ if, and only if, $W_0 = 0$. Concerning the system for x and y, we first discard the trivial case when no adults or nymphs are initially present, that is $x_0 = y_0 = 0$. Then, the only solution of system (3.4) is $(0, 0, W_0 e^{-\mu_W t})$, by (3.5), and the theorem holds trivially.

Let us then assume that not both $x_0 = 0$ and $y_0 = 0$ are true. We will prove that, in this case, $x(t), y(t) > 0$ for all $t > 0$, so that *a fortiori* y is bounded away from $-\nu$. Note that if either $x_0 = 0$ or $y_0 = 0$ (but not both), then the derivative of that which is initially zero is positive and, therefore, for all $t > 0$ *small enough*, by continuity, both $x(t)$ and $y(t)$ will be positive. Hence, we may assume, without loss of generality, that $x_0 > 0$ and $y_0 > 0$. Using an integrating factor to solve explicitly for y as a function of x in system (3.4),

$$y(t) = y_0\, e^{-\int_0^t \left(\mu_N + \gamma + \xi W(s)\right) ds} + \rho \int_0^t e^{-\int_\tau^t \left(\mu_N + \gamma + \xi W(s)\right) ds} x(\tau)\, d\tau. \tag{3.6}$$

Suppose now that x and y do not remain positive for all time and let t_0 be the first positive time for which either x or y vanish. Equation (3.6) proves that it is not possible that $y(t_0) = 0$ because then it would necessarily exist $\bar{t} \in (0, t_0)$ for which $x(\bar{t}) = 0$, contradicting the definition of t_0. Therefore, $x(t_0) = 0$, $y(t_0) > 0$, and $\bar{y} = \min\{y(t)\colon t \in [0, t_0]\} > 0$ by continuity and definition of t_0. Because x is continuous and $x(t_0) = 0$, there exists $h > 0$ such that $x(t) < \min\left\{\frac{\gamma \bar{y}}{\mu_A + \frac{C_A}{B}}, 1\right\}$ for all $t \in [t_0 - h, t_0]$. But then Equation (3.4) implies that $x'(t) > \gamma \bar{y} - \left(\mu_A + \frac{C_A}{B}\right)x(t) > 0$ for all $t \in [t_0 - h, t_0]$ and, because $x(t) > 0$ for all $t \in (t_0 - h, t_0)$, it is impossible for $x(t_0)$ to vanish, contradicting our assumption. Consequently, x and y remain positive por all time.

□

 doi:10.20944/preprints202601.0045.v1

3.1.2. Steady States of the System

The steady states of the system (3.4) are the solutions $(\bar{x}, \bar{y}, \overline{W}) \in \mathbb{R}^3_+$ of the following quadratic algebraic system:

$$\gamma y - \left(\mu_A + \frac{C_A}{B}x\right)x = 0, \tag{3.7}$$

$$\rho x - (\mu_N + \gamma + \xi W)y = 0, \tag{3.8}$$

$$\xi\left(\frac{y}{\nu + y}\right)W - \mu_W W = 0. \tag{3.9}$$

It follows from (3.8) that

$$\bar{x} = 0 \iff \bar{y} = 0. \tag{3.10}$$

We see from (3.9) that

$$\overline{W} = 0 \qquad \text{or} \qquad \bar{y} = \frac{\mu_W \nu}{\xi - \mu_W}. \tag{3.11}$$

Next, Equations (3.7) and (3.8) imply that

$$\bar{y} = \left(\frac{\mu_A}{\gamma} + \frac{C_A}{\gamma B}\bar{x}\right)\bar{x} \qquad \text{and} \qquad \bar{y} = \left(\frac{\rho}{\gamma + \mu_N + \xi\overline{W}}\right)\bar{x}, \tag{3.12}$$

whereby

$$\bar{x} = 0 \qquad \text{or} \qquad \bar{x} = \frac{\gamma B}{C_A}\left(\frac{\rho}{\gamma + \mu_N + \xi\overline{W}} - \frac{\mu_A}{\gamma}\right). \tag{3.13}$$

We can establish the following results concerning the equilibrium points of the system (3.4).

Theorem 3. *There are two equilibria without T. radiata: the extinction equilibrium*

$$E_0 = (0, 0, 0), \tag{3.14}$$

and a unique "no-T. radiata" equilibrium

$$E_W = (\hat{x}, \hat{y}, 0),\ \hat{x} > 0, \hat{y} > 0. \tag{3.15}$$

Proof. It follows from (3.9) and (3.10) that the only steady state with $\bar{x} = 0$ or $\bar{y} = 0$ is E_0. Also, (3.12) and (3.13) imply that a steady state of the form (3.15) must have

$$\boxed{\hat{x} = \frac{\gamma B}{C_A}\left(\frac{\rho}{\gamma + \mu_N} - \frac{\mu_A}{\gamma}\right) \qquad \text{and} \qquad \hat{y} = \frac{\gamma\rho B}{C_A(\gamma + \mu_N)}\left(\frac{\rho}{\gamma + \mu_N} - \frac{\mu_A}{\gamma}\right)}, \tag{3.16}$$

where the basic reproduction number for *D. citri* must be larger than 1:

$$\mathscr{R}_0^D := \frac{\rho\gamma}{\mu_A(\gamma + \mu_N)} > 1. \tag{3.17}$$

□

Note that this basic reproduction number is the product of the expected number of nymphs that a *D. citri* adult will produce, $\frac{\rho}{\gamma + \mu_N}$ and the expected number of adults that those nymphs will develop into, $\frac{\gamma}{\mu_A}$.

 doi:10.20944/preprints202601.0045.v1

Concerning coexistence steady states, we see from (3.7) that, for any steady state $(\bar{x}, \bar{y}, \overline{W})$ with $\bar{x} \neq 0$ and $\bar{y} \neq 0$,

$$\bar{y} = \frac{1}{\gamma}\left(\mu_A + \frac{C_A}{B}\bar{x}\right)\bar{x},$$

which is equivalent to

$$\frac{\bar{x}}{\bar{y}} = \frac{\gamma}{\mu_A + \frac{C_A}{B}\bar{x}}, \tag{3.18}$$

and in turn, equivalent to

$$\rho\frac{\bar{x}}{\bar{y}} - (\gamma + \mu_N) = \frac{\rho\gamma}{\mu_A + \frac{C_A}{B}\bar{x}} - (\gamma + \mu_N) = (\gamma + \mu_N)\left(\frac{\rho\gamma}{\mu_A(\gamma + \mu_N) + \frac{C_A(\gamma+\mu_N)}{B}\bar{x}} - 1\right). \tag{3.19}$$

Finally, we can describe the coexistence equilibrium that requires the *T. radiata* basic reproduction number to be larger than 1:

$$\mathscr{R}_0^T := \frac{\xi}{\mu_W} > 1. \tag{3.20}$$

.

Theorem 4. *Let* $\mathscr{R}_0^T > 1$, *let* $\bar{y} = \frac{\mu_W \nu}{\xi - \mu_W}$, *and* $\bar{x} = \frac{\sqrt{(\mu_A B)^2 + 4BC_A\gamma\bar{y}} - \mu_A B}{2C_A}$. *If* $\mathscr{R}_0^D > 1 + \frac{C_A\bar{x}}{B\mu_A}$, *there exists a unique coexistence equilibrium*

$$E^* = (x^*, y^*, W^*), \quad \textit{with} \quad x^*, y^*, W^* > 0. \tag{3.21}$$

Proof. It follows respectively from (3.7), (3.11), and (3.8) that

$$\boxed{x^* = \frac{\sqrt{(\mu_A B)^2 + 4BC_A\gamma y^*} - \mu_A B}{2C_A}, \quad y^* = \frac{\mu_W \nu}{\xi - \mu_W}, \quad W^* = \frac{1}{\eta\xi}\left(\frac{\rho x^*}{y^*} - \gamma - \mu_N\right)}, \tag{3.22}$$

where x^* in (3.22) is positive if y^* is, while y^* in (3.22) is positive if, and only if, $\mathscr{R}_0^T > 1$. Finally, W^* in (3.22) is positive if, and only if, $\rho\gamma > \mu_A(\gamma + \mu_N) + \frac{C_A(\gamma+\mu_N)}{B}x^*$ because of (3.19), or equivalently, $\frac{\rho\gamma}{\mu_A(\gamma+\mu_N)} = \mathscr{R}_0^D > 1 + \frac{C_A x^*}{B\mu_A}$. □

3.1.3. Local Stability of Equilibrium Points

We shall now study the stability properties of these steady states by linearizing system (3.4) about each steady state.

The Jacobian matrix of the flow of system (3.4) is

$$J(x, y, W) = \begin{pmatrix} -\mu_A - 2\frac{C_a}{B}x & \gamma & 0 \\ \rho & -\mu_N - \gamma - \xi W & -\xi y \\ 0 & \frac{\xi\nu W}{(\nu+y)^2} & \frac{\xi y}{\nu+y} - \mu_W \end{pmatrix}. \tag{3.23}$$

We begin with the extinction steady state, E_0.

Theorem 5. *The extinction equilibrium is locally asymptotically stable if* $\mathscr{R}_0^D < 1$ *and unstable if* $\mathscr{R}_0^D > 1$.

Proof. We see from (3.23) that

$$J(E_0) = \begin{pmatrix} -\mu_A & \gamma & 0 \\ \rho & -\mu_N - \gamma & 0 \\ 0 & 0 & -\mu_W \end{pmatrix} \tag{3.24}$$

 doi:10.20944/preprints202601.0045.v1

has eigenvalues $-\mu_W$ and the two roots of $\lambda^2 + (\mu_A + \mu_N + \gamma)\lambda + \mu_A(\mu_N + \gamma) - \rho\gamma = 0$, which has two roots with negative real part if, and only if, its coefficients are positive. This is equivalent to $\mu_A(\mu_N + \gamma) - \rho\gamma > 0$, that is

$$\mathscr{R}_0^D = \frac{\rho\gamma}{\mu_A(\gamma + \mu_N)} < 1.$$

Similarly, when $\mathscr{R}_0^D > 1$, the characteristic equation has two real roots, one negative and the other positive, making the equilibrium unstable and finishing our proof.

□

Next we turn to the stability of the "no-*T. radiata*" steady state.

Theorem 6. *Let $\mathscr{R}_0^D > 1$ so that E_W exists. Then, E_W is LAS if $\mathscr{R}_0^T < 1 + \frac{\nu}{\hat{y}}$ and it is unstable if $\mathscr{R}_0^T > 1 + \frac{\nu}{\hat{y}}$.*

Proof. The Jacobian matrix (3.23) at the equilibrium E_W is

$$J(E_W) = \begin{pmatrix} \mu_A - 2\frac{\gamma\rho}{\gamma+\mu_N} & \gamma & 0 \\ \rho & -\mu_N - \gamma & -\xi\hat{y} \\ 0 & 0 & \frac{\xi\hat{y}}{\nu+\hat{y}} - \mu_W \end{pmatrix}, \tag{3.25}$$

with eigenvalues

$$\lambda_1 = \frac{\xi\hat{y}}{\nu + \hat{y}} - \mu_W \tag{3.26}$$

and the two roots of

$$\lambda^2 + \left(\gamma + \mu_N + \frac{2\gamma\rho}{\gamma + \mu_N} - \mu_A\right)\lambda + \gamma\rho - \mu_A(\gamma + \mu_N) = 0. \tag{3.27}$$

The discriminant of this quadratic is positive:

$$\left(\gamma + \mu_N + \tfrac{2\gamma\rho}{\gamma+\mu_N} - \mu_A\right)^2 - 4(\gamma\rho - \mu_A(\gamma + \mu_N)) = \left(\frac{2\gamma\rho}{\gamma + \mu_N} - \mu_A\right)^2 + (\gamma + \mu_N)^2 + 2\mu_A(\gamma + \mu_N),$$

and hence both its roots are real. Because $\mathscr{R}_0^D > 1$, all the coefficients of (3.27) are positive, making both its roots negative. Finally, it follows from (3.26) that a necessary and sufficient additional condition for E_W to be locally asymptotically stable is $\frac{\xi\hat{y}}{\nu+\hat{y}} < \mu_W$, which is automatic if $\mathscr{R}_0^T \leq 1$. In any case, this condition is equivalent to $\frac{\xi}{\mu_W} < 1 + \frac{\nu}{\hat{y}}$ and the theorem is proved.

□

We finally turn to the stability of E^*.

Theorem 7. *Let $\mathscr{R}_0^T > 1$ and $\mathscr{R}_0^D > 1 + \frac{C_A x^*}{B\mu_A}$. Then, the coexistence equilibrium E^* is locally asymptotically stable.*

Proof. The Jacobian matrix (3.23) at the coexistence equilibrium is

$$J(E^*) = \begin{pmatrix} -d_1 & \gamma & 0 \\ \rho & -\rho\frac{x^*}{y^*} & -\xi y^* \\ 0 & \frac{\xi\nu W^*}{(\nu+y)^2} & 0 \end{pmatrix}, \tag{3.28}$$

where $d_1 = \sqrt{\mu_A^2 + \frac{4\gamma C_A y^*}{B}}$. The characteristic polynomial is

$$\lambda^3 + p_2\lambda^2 + p_1\lambda + p_0,$$

 doi:10.20944/preprints202601.0045.v1

where

$$p_2 = d_1 + \rho\,\frac{x^*}{y^*} > 0, \qquad p_1 = \rho\,\frac{x^*}{y^*}\,d_1 + \frac{\xi\mu_W \nu W^*}{\nu + y^*} - \rho\gamma, \qquad p_0 = d_1\,\frac{\xi\mu_W \nu W^*}{\nu + y^*} > 0. \tag{3.29}$$

In order to prove that all eigenvalues have negative real part, we shall use the Routh-Hurwitz criterion: $p_2 > 0$, and $0 < p_0 < p_1 p_2$. We just need to prove that $p_0 < p_1 p_2$. We see that

$$p_0 < p_1 p_2 \iff 0 < d_1\left(\rho\,\frac{x^*}{y^*}\,d_1 - \rho\gamma\right) + \rho\,\frac{x^*}{y^*}\left(\rho\,\frac{x^*}{y^*}\,d_1 + \frac{\xi\mu_W \nu W^*}{\nu + y^*} - \rho\gamma\right), \tag{3.30}$$

and it suffices to show that $\dfrac{x^*}{y^*}\,d_1 > \gamma$. Using (3.18), it follows that

$$\begin{aligned}
\frac{x^*}{y^*}\,d_1 > \gamma \quad &\iff \quad d_1^2 = \mu_A^2 + \frac{4\gamma C_A y^*}{B} > \left(\frac{\gamma y^*}{x^*}\right)^2 = \left(\mu_A + \frac{C_A}{B}x^*\right)^2 \\
&\iff \quad 4\gamma y^* > 2\mu_A x^* + \frac{C_A}{B}(x^*)^2 \iff 4\,\frac{\gamma y^*}{x^*} > 2\mu_A + \frac{C_A}{B}\,x^* \\
&\iff \quad 4\left(\mu_A + \frac{C_A}{B}\,x^*\right) > 2\mu_A + \frac{C_A}{B}\,x^*,
\end{aligned}$$

thus finishing the proof. □

Remark. It follows from Theorems 6 and 7 that, if both conditions $1 < \mathscr{R}_0^T < 1 + \frac{\nu}{\hat{y}}$ and $\mathscr{R}_0^D > 1 + \frac{C_A x^*}{B\mu_A}$ hold, then both equilibrium points E_W and E^* would be locally asymptotically stable. However, those conditions cannot hold simultaneously. In fact, we have

Theorem 8. *Let $\mathscr{R}_0^T > 1$. Then, $\mathscr{R}_0^T < 1 + \frac{\nu}{\hat{y}} \iff \mathscr{R}_0^D < 1 + \frac{C_A x^*}{B\mu_A}$.*

Proof. It follows from (3.15), (3.20), and (3.22) that

$$\mathscr{R}_0^T < 1 + \frac{\nu}{\hat{y}} \iff y^* = \frac{\nu}{\mathscr{R}_0^T - 1} > \hat{y} = \frac{\rho B \mu_A}{C_A(\gamma + \mu_N)}\left(\mathscr{R}_0^D - 1\right). \tag{3.31}$$

Also, it follows from (3.17) and (3.22) that

$$\begin{aligned}
\mathscr{R}_0^D > 1 + \frac{C_A x^*}{B\mu_A} \quad &\iff \quad \left(\frac{2\gamma\rho}{\mu_A(\gamma + \mu_N) - 1}\right)^2 > 1 + \frac{4\gamma\nu C_A}{B\mu_A^2(\mathscr{R}_0^T - 1)} \\
&\iff \quad \frac{\rho^2\gamma}{(\gamma + \mu_N)^2} = \frac{\rho\mu_A \mathscr{R}_0^D}{\gamma + \mu_N} > \frac{\rho\mu_A}{\gamma + \mu_N} + \frac{\nu C_A}{B(\mathscr{R}_0^T - 1)} \\
&\iff \quad \frac{\rho\mu_A}{\gamma + \mu_N}\left(\mathscr{R}_0^D - 1\right) > \frac{\nu C_A}{B(\mathscr{R}_0^T - 1)}.
\end{aligned} \tag{3.32}$$

The theorem now follows from (3.31) and (3.32).

□

3.1.4. Global Stability of the Trivial Equilibrium

We can establish global stability conditions for the trivial equilibrium (3.4).

Theorem 9. *If $\mathscr{R}_0^D < 1$ and $\mathscr{R}_0^T < 1$, the extinction equilibrium, $E_0 = (0, 0, 0)$ is globally asymptotically stable in the positive octant, $\mathbb{R}^3_+$.*

 doi:10.20944/preprints202601.0045.v1

Proof. Consider the linear Lyapunov function

$$V(x,y,W) = a_1 x + a_2 y + a_3 W, \quad a_i > 0, \quad i = 1,2,3.$$

Each term of $V(x,y,W)$ is nonnegative for $(x,y,W) \in \mathbb{R}^3_+ \setminus \{E_0\}$ when $a_1, a_2, a_3 \geq 0$. Differentiating V along the trajectories of system (3.4) yields

$$\dot{V} = a_1\left[\gamma\, y - \mu_A x - \frac{C_A}{B}\, x^2\right] + a_2\left[\rho\, x - (\mu_N + \gamma + \xi\, W)\, y\right] \quad + a_3\left[\frac{\xi\, y}{\nu + y} W - \mu_W\, W\right]. \tag{3.33}$$

Regrouping the terms in (3.33),

$$\dot{V} = \underbrace{\left(-a_1\mu_A + a_2\rho\right)}_{\text{coef. of } x}\, x \;+\; \underbrace{\left(a_1\gamma - a_2(\mu_N + \gamma + \xi\, W)\right)}_{\text{coef. of } y}\, y \;-\; a_1\frac{C_A}{B}\, x^2 \\ +a_3\left[\frac{\xi\, y}{\nu + y} - \mu_W\right] W. \tag{3.34}$$

Let

$$a_2 = \frac{a_1\, \mu_A}{\rho} > 0,$$

so that the linear x-term in (3.34) vanishes. Thus,

$$\dot{V} = a_1\gamma\left[1 - \frac{\mu_A(\mu_N + \gamma + \xi\, W)}{\rho\gamma}\right] y \;-\; a_1\frac{C_A}{B}\, x^2 \;+\; a_3\left[\frac{\xi\, y}{\nu + y} - \mu_W\right] W. \tag{3.35}$$

Define

$$k_1 := a_1\gamma\left(\tfrac{\mu_A(\mu_N+\gamma)}{\rho\gamma} - 1\right), \quad k_2 := a_1\tfrac{C_A}{B}, \quad k_3 := a_3(\mu_W - \xi).$$

Note that:

- Since $R_0^D < 1$ is equivalent to $\frac{\mu_A(\mu_N+\gamma)}{\rho\gamma} > 1 \implies a_1\gamma\left(\frac{\mu_A(\mu_N+\gamma)}{\rho\gamma} - 1\right) = k_1 > 0$
- $a_1, C_A, B > 0 \implies a_1\frac{C_A}{B} = k_2 > 0$
- Also, because $R_0^T = \frac{\xi}{\mu_W} < 1$ we have $\mu_W - \xi > 0 \implies a_3(\mu_W - \xi) = k_3 > 0$.
  Use monotonicity bounds:
  $\mu_N + \gamma + \xi\, W \geq \mu_N + \gamma \implies 1 - \frac{\mu_A(\mu_N + \gamma + \xi\, W)}{\rho\gamma} \leq 1 - \frac{\mu_A(\mu_N + \gamma)}{\rho\gamma} = -\frac{k_1}{a_1\gamma}$
  Also
  $\frac{y}{\nu + y} < 1 \implies \xi\frac{y}{\nu + y} - \mu_W \leq \xi - \mu_W = -(\mu_W - \xi)$
  Therefore,
  $$\dot{V} \leq -k_1\, y - k_2\, x^2 - k_3\, W \leq 0.$$

The largest invariant set where $\dot{V} = 0$ is exactly $E_0 = (0,0,0)$. By LaSalle's invariance principle, every trajectory with nonnegative initial conditions converges to E_0. Hence E_0 is globally asymptotically stable in $\mathbb{R}^3_+$.
□

3.2. Simulations

3.2.1. Reduced System

For our first simulations, corresponding to the reduced system (3.4), we use the parameter values displayed in Table 2, estimated from the literature or within a biologically relevant range —with the exception of some tree-related parameters that were set to zero to ensure a constant total number of

 doi:10.20944/preprints202601.0045.v1

shoots as required in (3.4). We then modify the values of some of the parameters so that they fall under the ranges of Theorems 5–7.

Table 2. Parameter values for simulating the reduced *D. citri–T. radiata* model

Parameter	Value	Parameter	Value
ρ	6.52×10^{-2}	C_A	2.07×10^{-5}
μ_A	$1/32$	μ_N	$1/6$
γ	$1/6.11$	μ_W	0.04
ξ	2	ν	200

.

These result in the following basic reproduction numbers:
$\mathscr{R}_0^T > 1$ and $\mathscr{R}_0^D > 1$,
which correspond to Theorem (7). We ran a 60-year simulation using the following initial conditions:

Table 3. Initial values for the reduced *D. citri–T. radiata* model.

Variable	Initial Value
$N(0)$	30
$A(0)$	0
$T_1(0)$	200
$T_2(0)$	100
$N_i(0)$	0.2
$A_i(0)$	150
$T_{1i}(0), T_{2i}(0)$	0
$W(0)$	1,000

The results of are displayed in Figures 1 and 2, clearly corroborating Theorem 7.

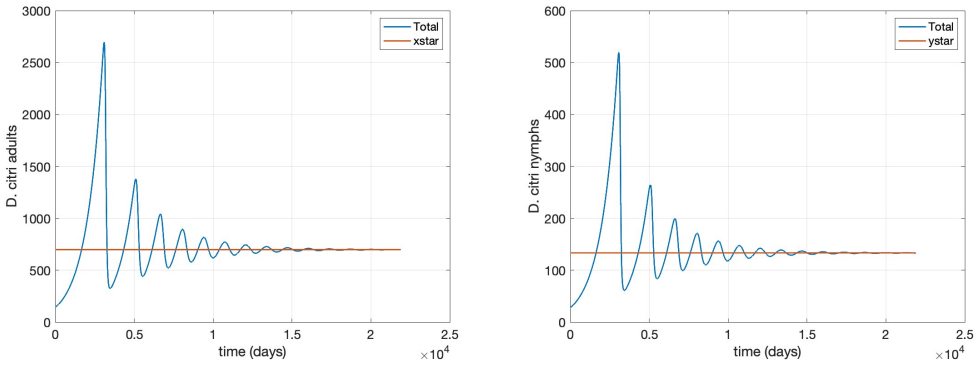

Figure 1. *D. citri* population and equilibrium values x^*, y^*.

Preprints.org (www.preprints.org) | NOT PEER-REVIEWED | Posted: 1 January 2026 doi:10.20944/preprints202601.0045.v1

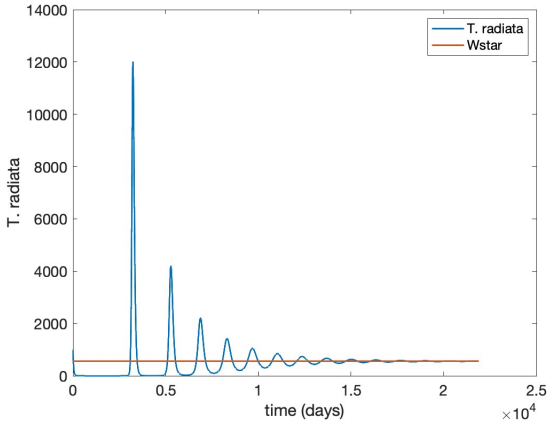

Figure 2. *T. radiata* population and equilibrium W^*.

Next, we modified the unit birth rate of *T. radiata* to $\xi = 0.041$ so its basic reproduction number is $\mathscr{R}_0^T = 1.025$ corresponding to Theorem (6), as corroborated in Figures 3 and 4.

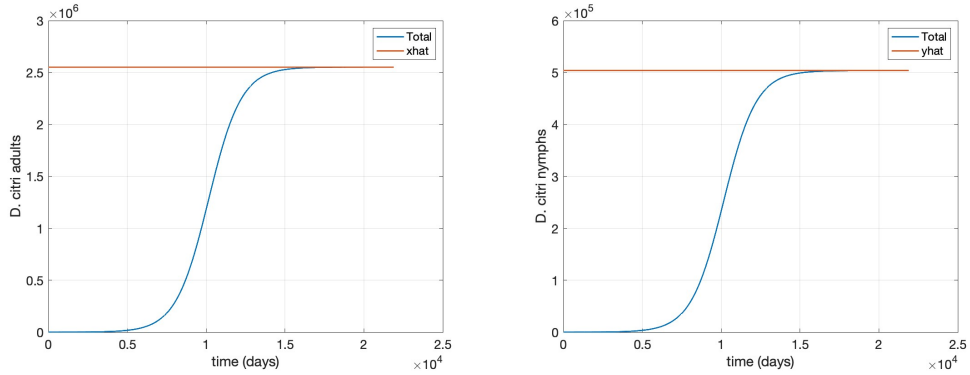

Figure 3. *D. citri* population and equilibrium $\hat{x}$, $\hat{y}$.

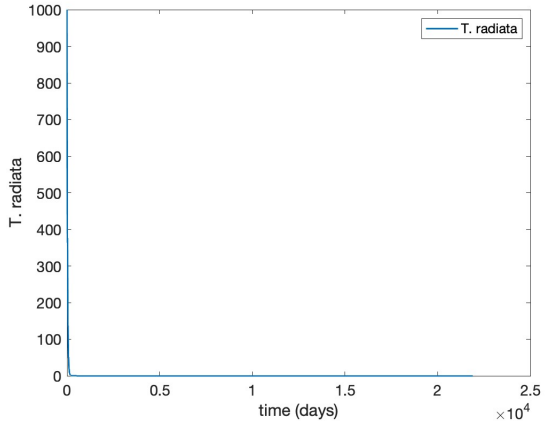

Figure 4. Total *T. radiata* population.

Finally, we restore $\xi = 0.1$ and slightly modify the value of the per capita "oviposition" rate for *D. citri* to $\rho = 0.0625$ to lower its basic reproduction number to $\mathscr{R}_0^D = 0.991$ that corresponds to Theorem (5), as corroborated below in Figures 5, and 6.

 doi:10.20944/preprints202601.0045.v1

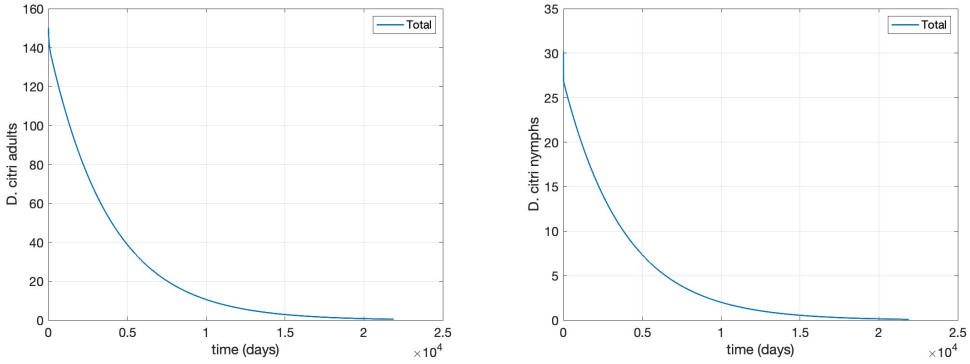

Figure 5. *D. citri* population extinction.

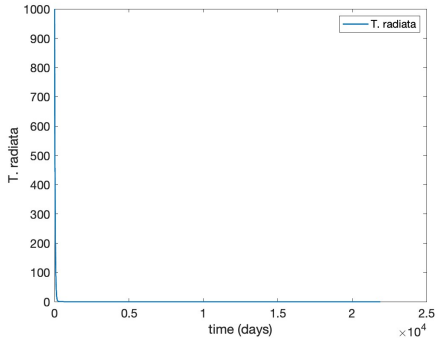

Figure 6. *T. radiata* population extinction.

3.2.2. Full System

Because the model (2.1)–(2.2) was designed for a real agricultural context, we considered several different scenarios to simulate potential management practices. For all of them we assume:

- No transition between low-productivity and high-productivity trees (or vice versa)
- No tree eradication
- Effectiveness of agrochemical decays linearly to zero 30 days after application

For our second set of simulations, corresponding to the system (2.1), we use the parameter values displayed in Table 4, estimated from the extant literature or chosen within a biologically relevant range. We ran a 1-year simulation using the initial conditions described in Table 5.

 doi:10.20944/preprints202601.0045.v1

Table 4. Parameter values for simulating the extended *D. citri*-*T. radiata* model.

Parameter	Value	Source
ρ	0.995	Estimated value from [11]
m_1	42	Estimated value from [12]
m_{1i}	32	Assumed from [12]
m_2	21	Assumed from [12]
m_{2i}	21/2	Assumed from [12]
μ_N	0.02	Estimated value from [12]
μ_A	1/(48.25)	Estimated value from [13]
μ_W	0.04	Estimated value from [14]
μ_{T_2}	1/(10*365)	Estimated value from [15]
$\mu_{T_{2i}}$	1/(5*365)	Estimated value from [16]
γ	1/9	Estimated value from [13]
ξ	25	Estimated value from [17]
C_A	2.07×10^{-5}	Assumed
θ_T	7.00×10^{-3}	[18]
τ	0	Assumed
λ, λ_i	0	Assumed
α_1, α_2	0	Assumed
ν	200	Assumed
η	10^{-6}	Assumed

Table 5. Initial values for the extended *D. citri*–*T. radiata* model.

Variable	Initial Value
$N(0)$	192
$A(0)$	214
$T_1(0)$	100
$T_2(0)$	43
$N_i(0)$	96
$A_i(0)$	107
$T_{1i}(0)$	100
$T_{2i}(0)$	42
$W(0)$	0

A total of 285 Tahiti acid lime trees (*Citrus* × *latifolia* Tanaka ex Q. Jiménez) are included, corresponding to standard planting density per hectare for Colombian cultivation [15]. The interventions we consider are one or both of releasing *T. radiata* and applying agrochemicals. Therefore, our simulation scenarios are the following four:

- **Scenario 1, No control:** (i.e., no management interventions)

$$\delta_N(t) = \delta_A(t) = \delta_W(t) = \Lambda(t) = 0\,, \forall t \geq 0.$$

 doi:10.20944/preprints202601.0045.v1

- **Scenario 2, *T. radiata* release only:** introduction of 400 females at the initial time, taking into account as a reference the prescribed release rates (individuals/ha, between male and female) [15], as shown in Figure **??**.
- **Scenario 3, Agrochemical application only:** ($\delta_N(t)$, $\delta_A(t)$, $\delta_W(t)$) shown in Figure **??**.
- **Scenario 4, Combined control:** pairing initial agrochemical application (see Figure **??**) with *T. radiata* release of 100 females at day 30 (see Figure **??**).

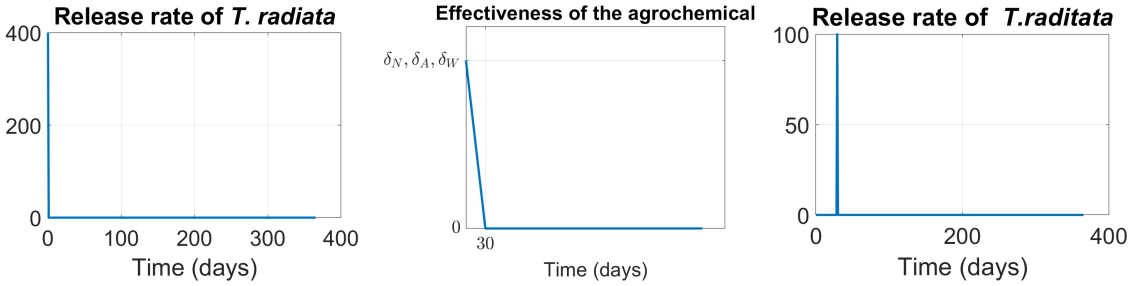

Figure 7. Functions modeling the interventions

The results of these simulation scenarios are shown in Figures 8, 9, and 10. In each of these figures, the right panels depict a zoom-in of the corresponding left panels near the origin to help understand the initial impact of the interventions, while the 1-year simulations displayed on the left panels are intended to show the long-term effect of the interventions. In Figure 8, we show the result of the simulations for the populations of uninfected *D. citri* nymphs and adults. In Figure 9, we show the result of the simulations for the populations of infected *D. citri* nymphs and adults. In Figure 10, we show the result of the simulations for the populations of *T. radiata* and for those of uninfected and infected trees. In all scenarios, the population of HLB-infected trees increases while the populations of uninfected and total trees decrease, because the model does not include any source for new healthy trees or recovery from HLB infection.

Scenario 1 serves as a baseline that underscores the devastating effect that HLB may have on the plantation (second panel of Figure 10). We see that after one year, the initial 142 infected trees would increase their numbers to 245 (72.5% increase), while the initial 143 uninfected trees would decrease to just 26 (81.8% decrease).

 doi:10.20944/preprints202601.0045.v1

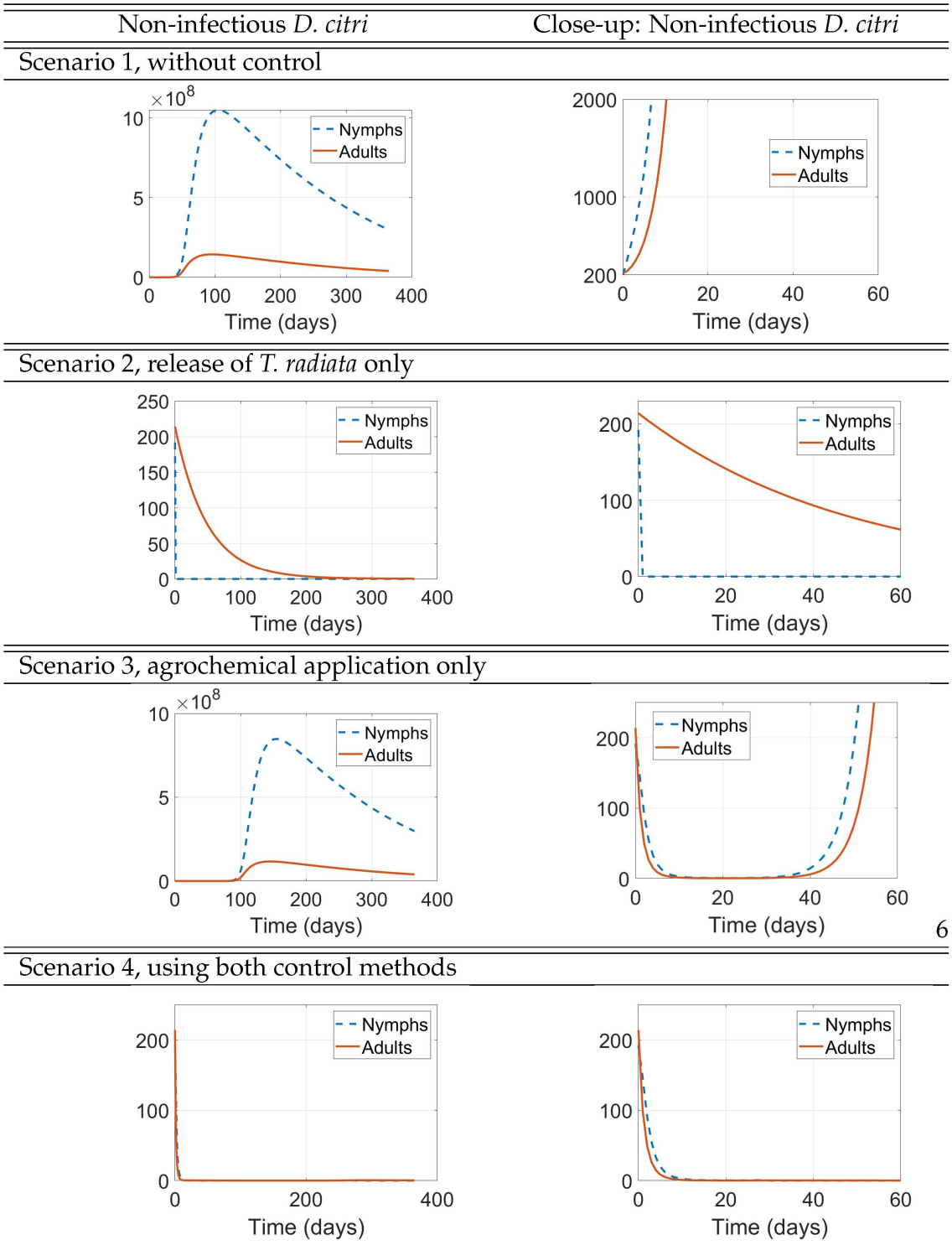

Figure 8. non-infectious *D. citri* populations

We see, in Figure 8 for the uninfected *D. citri* and in Figure 9 for the infectious *D. citri*, that just the release of 400 adult wasps of *T. radiata* when the *D. citri* nymph population is still small (here, one-half the number of released *T. radiata*, Scenario 2) results in a very quick extinction of the latter, in approximately 2 days in both figures (second panels of Scenario 2), which then depletes the *D. citri* adult population in about 8-9 months (first panels of Scenario 2), as well as the *T. radiata* population that cannot productively lay their eggs once the nymphs are depleted (first panel of Scenario 2 in Figure 10). After one year, this intervention is very successful in reducing the plantation's losses, by reducing

Preprints.org (www.preprints.org) | NOT PEER-REVIEWED | Posted: 1 January 2026 doi:10.20944/preprints202601.0045.v1

the proportional increase of infected trees from 72.5% when no control measures are implemented to 57.7%, as well as diminishing the 81.8% decrease in the number of uninfected trees to 66.4%.

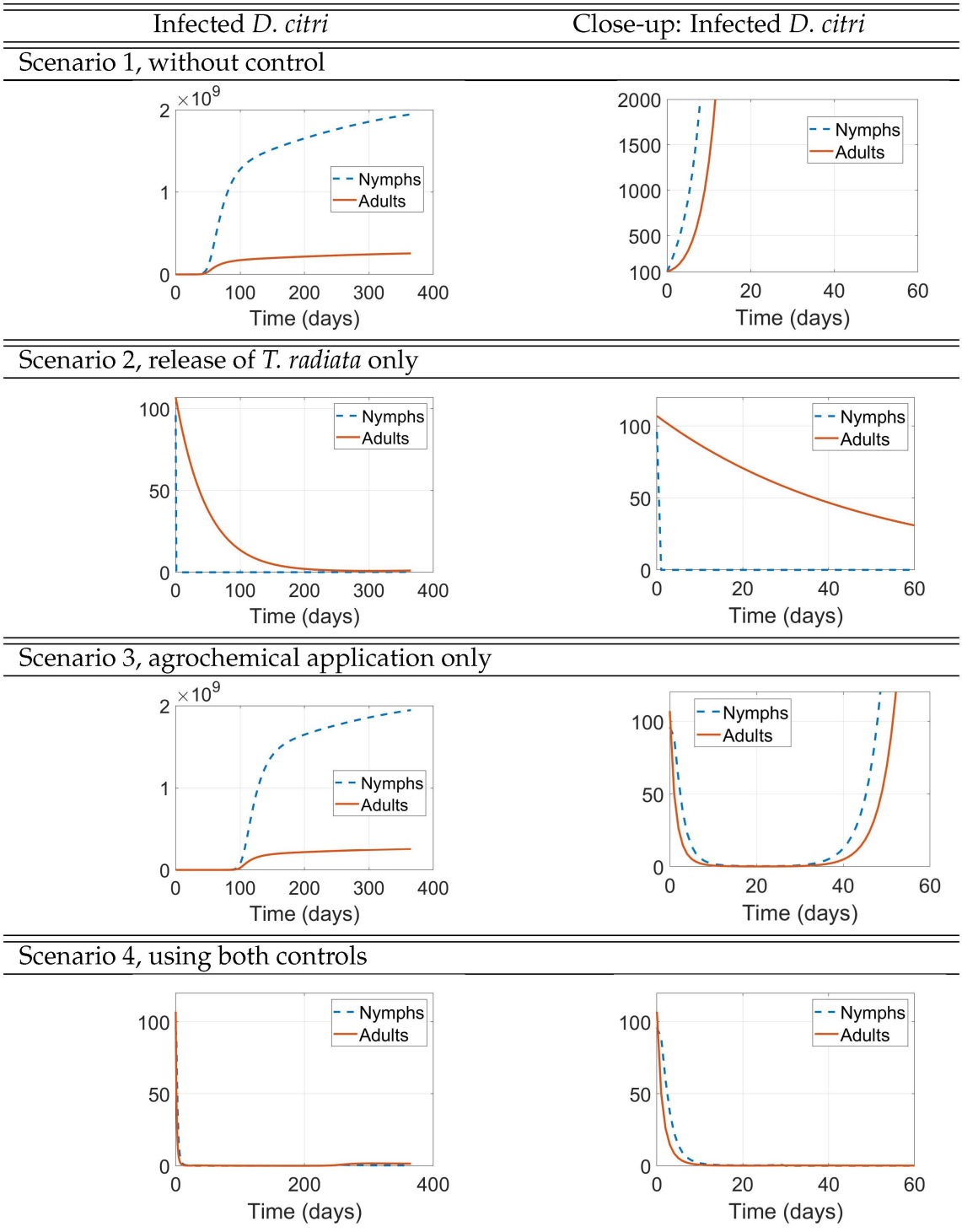

Figure 9. infected *D. citri* populations

On the other hand, we also see, in Figures 8 and 9, that just the application of an agrochemical of high initial effectiveness at that same time when the *D. citri* nymph population is still small (numbering 200, Scenario 3) *almost* leads to the extinction of the latter in the 30 days that the agrochemical is still effective (second panels of Scenario 2 in both figures) and, consequently, we also see the adult *D. citri* population being almost led to extinction. However, after those 30 days, the *D. citri* nymph population takes off to exceedingly large numbers that peak after about 5 months (first panels of Scenario 3 in

 doi:10.20944/preprints202601.0045.v1

both figures) by which time the population of uninfected trees has fallen to approximately half of its original number (second panel of Scenario 3 in Figure 10), causing the decline of both nymph and adult populations of *D. citri* to decrease.

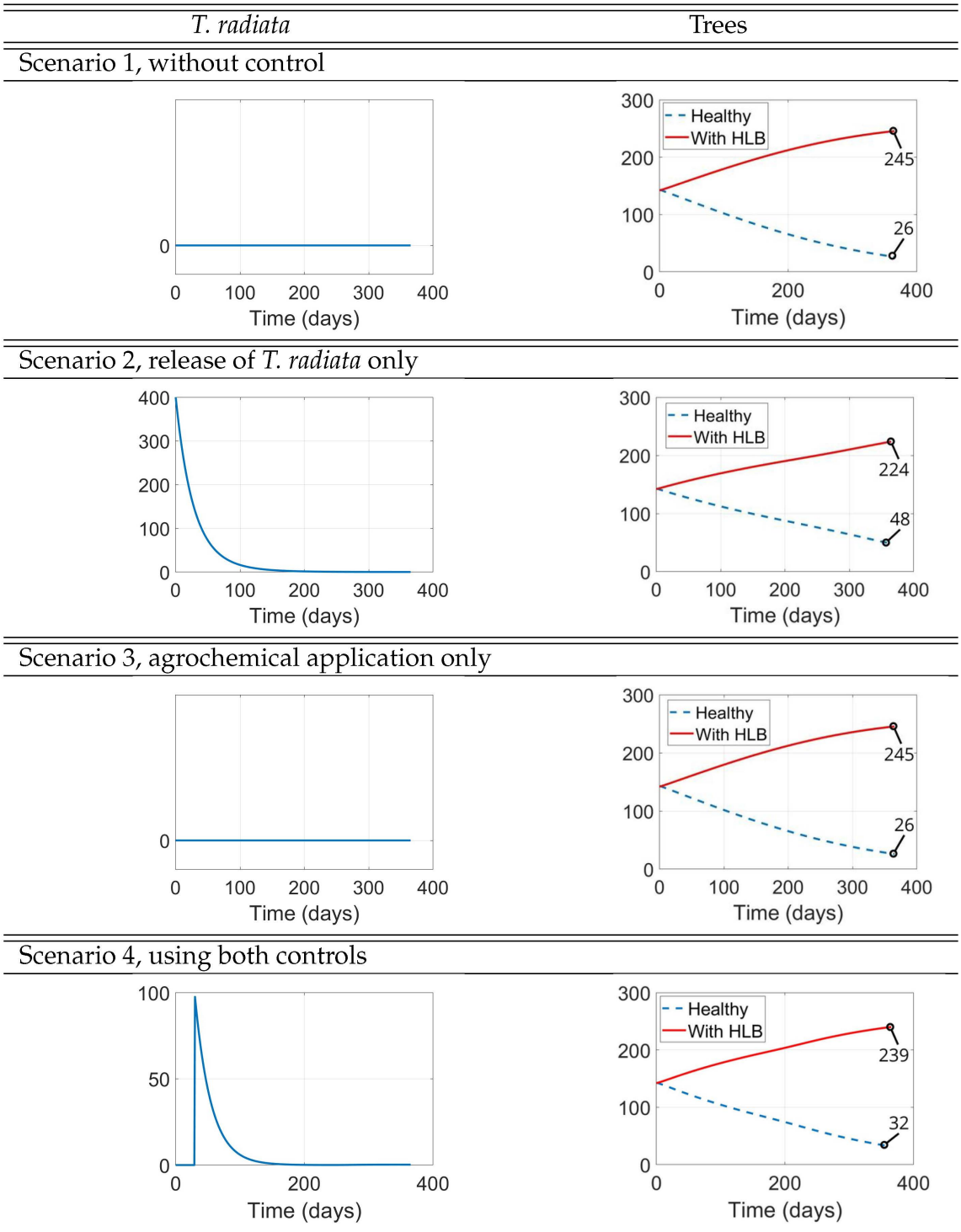

Figure 10. *T. radiata* and tree populations

In Scenario 4, we considered the sequential use of both control measures rather than their combined used simultaneously, with the release of *T. radiata* 30 days after the application of agrochemicals, to avoid considering the negative impact that the use of the latter has on the population of the former (because we assume that the effectiveness of the agrochemical is negligible after 30 days). In this scenario the realease of *T. radiata* involves just 100 adult wasps, instead of the 400 used in Scenario

 doi:10.20944/preprints202601.0045.v1

2. Yet, their timely release when the populations of *D. citri* had been decimated by the agrochemical, is enough to "finish the job". In fact, at day 30 in Scenario 4, the ratio of *T. radiata* to *D. citri* nymphs is considerably larger than the 2:1 ratio at the start of Scenario 2, thus making the wasps much more effective in extinguishing the *D. citri* population (and henceforth self-eliminating too!).

Comparing the second panels of Scenarios 3 and 4 in Figures 8 and 9, we see that the plots are identical during the first 30 days because the two scenarios are actually the very same during those 30 days. However, the delay in the release of the wasps when compared to Scenario 2, as expected, still significantly improves the results after one year in Scenario 3, both in terms of the numbers of healthy and infected trees and in the *D. citri* populations but cannot match the outcomes of Scenario 2, either for the trees or for the psyllyd populations.

The seeming resurgence of *D. citri* adults after approximately 2-3 months (first panel of Figure 9, Scenarios 1 and 3) is a numerical artifact due to the positivity of solutions of our ODE system and the increased number of infected trees upon whose shoots the adult psyllid feeds and lays eggs.

4. Discussion

We proposed a 9-dimensional ODE model to describe the dynamics of interactions and infection of *D. citri*, *T. radiata*, and lemon trees with the bacterium Huanlongbing. The model incorporates control interventions by agrochemicals (pesticides to contain the *D. citri* population) and by the parasitoid of *D. citri*, *T. radiata*.

We reduced the system to a 3-dimensional system that omits the dynamics of the tree population and combines uninfected and infected populations of *D. citri*. That is, the reduced model described the dynamics of interaction of *D. citri* with its parasitoid *T. radiata*.

For the reduced system we carried out a fairly complete mathematical analysis of well-posedness and long term dynamics. We proved that, for non-negative initial conditions, the intial value problem has a unique, non-negative, global-in-time solution that converges asymptotically to one of three equilibrium points of the system. The asymptotic behavior is determined by the two basic reproduction numbers of the interacting populations in threshold form.

We found explicit expressions for the only three biologically relevant equilibrium points, one being the extinction equilibrium, a second one, the "no-*Tamarixia*-equilibrium" (a boundary equilibrium, with positive *D. citri* population but no *T. radiata*), and a coexistence equilibrium.

We provided explicit formulas for $\mathcal{R}_0^D$, the basic reproduction number for the *D. citri* population, and for $\mathcal{R}_0^T$, the basic reproduction number for the *T. radiata* population. We proved that the local asymptotic stability of equilibria operates exactly as one would expect: when both basic reproduction numbers are smaller than 1, the extinction equilibrium is the only one in the non-negative octant, and it is locally asymptotically stable. As $\mathcal{R}_0^D$ increases from below to above 1, the "no-*Tamarixia*-equilibrium", E_W, bifurcates from the extinction equilibrium into the non-negative octant and it is locally asymptotically stable as long as $\mathcal{R}_0^T$ is smaller than an explicitly computable critical value that is larger than 1. As $\mathcal{R}_0^T$ increases from below that critical value to above it, E_W becomes unstable and the coexistence equilibrium (which bifurcated from E_W when $\mathcal{R}_0^T$ crossed from below to above 1) becomes locally asymptotically stable.

We also proved global stability of the trivial equilibrium via Lyapunov functions and LaSalle's invariance principle, establishing that the threshold conditions for local asymptotic stability actually result in global stability within the non-negative octant of $\mathbb{R}^3$.

We performed simulations of the full 9-dimensional model in four scenarios, to get a sense of the impact of the two types of control measures. The first scenario is without control and serves as a baseline. The second one introduces *T. radiata* only while the third one uses only one application of a high-efficiency agrochemical pesticide. The last scenario uses the agrochemical first, followed by the release of a reduced number of *T. radiata* after 30 days, which is the estimated duration of the pesticide's effect.

 doi:10.20944/preprints202601.0045.v1

Based on the simulations, it seems that the preferred control method is *T. radiata*, but a further cost anaylisis needs to be performed. The reason that *T. radiata* is so effective hinges upon its mode of reproduction. The fact that they lay one egg into a *D. citri* nymph that will not evolve to adulthood, makes this wasp species highly effective in controlling –and even eliminating– the *D. citri* population.

Author Contributions: Conceptualization, S.F., F.M. and L.S.; methodology, F.M. and L.S.; software, S.F.; validation, S.F., F.M. and L.S.; formal analysis, F.M.; investigation, S.F.; resources, S.F.; data curation, S.F., F.M. and L.S.; writing—original draft preparation, S.F., F.M. and L.S.; visualization, S.F.; supervision, L.S.; project administration, L.S.; funding acquisition, L.S.

Funding: This research was funded in part by the Colombian Ministry of Science, Technology and Innovation (MinCiencias) grant number 933-2023.

Acknowledgments: The authors wish to express their gratitude for contributions and support provided by collaborating institutions and individuals, including: to the MoBiMat Center for technical support and discussions; to the Colombian Corporation for Agricultural Research (AGROSAVIA) –especially to Dr. Lumey Pérez-Artiles, MSc., Ms. Madeleyne Parra-Fuentes, Dr. Takumasa Kondo, Dr. Juan Humberto Guarín and their research teams; to UNESP Botucatu, Brazil –particularly to Drs. Claudia Pio and Helenice Silva; to the Institute of Agricultural Science ICA - CSIC, Spain, –especially to Dr. Alberto Fereres Castiel and his research team; to the Colombian Horticultural Association (ASOHOFRUCOL) –particularly to the Director of the Magdalena Chapter, Ramiro Salcedo; to the Secretariat of Economic Development of Magdalena, Colombia; and to the citrus growers from the departments of Atlántico, Magdalena, Cauca and Valle del Cauca.

Conflicts of Interest: The authors declare no conflicts of interest.

Abbreviations

The following abbreviations are used in this manuscript:

HLB	Huanglongbin
CLas	*Candidatus* Liberibacter asiaticus

References

1. Aguirre, A.; Giancola, S.; Gochez, A. Manejo del complejo HLB-vector en regiones citrícolas afectadas en centro y sudamérica. Technical report, FONTAGRO, 2025.
2. Gottwald, T.R. Current epidemiological understanding of citrus huanglongbing. *Annual Review of Phytopathology* **2010**, *48*, 119–139. https://doi.org/10.1146/annurev-phyto-073009-114418.
3. Li, S.; Wu, F.; Duan, Y.; Singerman, A.; Guan, Z. Citrus greening: Management strategies and their economic impact. *HortScience* **2020**, *55*, 604–612. https://doi.org/10.21273/HORTSCI14696-19.
4. Villar-Luna, H.; Santos-Cervantes, M.E.; Rodríguez-Negrete, E.A.; Méndez-Lozano, J.; Leyva-López, N.E. Economic and Social Impact of Huanglongbing on the Mexico Citrus Industry: A Review and Future Perspectives, 2024. https://doi.org/10.3390/horticulturae10050481.
5. de Agricultura, M.; (ICA), I.C.A. PLAN DE ACCIÓN NACIONALPARA EL HLB DE LOS CÍTRICOS 2019-2022. In Proceedings of the Mesa temática nacional del huamglomgbinb de los cítricos, 2019, pp. 1–49.
6. Kondo, T.; Riaño, N.M.; Pérez-Artiles, L.; Martínez, M.F.; Ríos-Rojas, L.; Fuentes, M.P.; Guarín, J.H.; Carabalí-Muñoz, A.; Orduz-Rodríguez, J.O.; Urquiza, G.P.C.; et al. *Avances en el conocimiento y recomendaciones para el manejo integrado de la enfermedad Huanglongbing (HLB) en los cultivos de cítricos en Colombia*; Corporación Colombiana de Investigación Agropecuaria (Agrosavia), 2024. https://doi.org/10.21930/agrosavia.analisis.7407846.
7. Chen, X.; Wong, S.W.; Stansly, P.A. Functional Response of Tamarixia radiata (Hymenoptera: Eulophidae) to Densities of Its Host, Diaphorina citri (Hemiptera: Psylloidea). *Annals of the Entomological Society of America* **2016**, *109*, 432–437. https://doi.org/10.1093/aesa/saw018.
8. Ammar, E.D.; Ramos, J.E.; Hall, D.G.; Dawson, W.O.; Shatters, R.G. Acquisition, replication and inoculation of Candidatus Liberibacter asiaticus following various acquisition periods on huanglongbing-infected citrus by nymphs and adults of the asian citrus psyllid. *PLoS ONE* **2016**, *11*. https://doi.org/10.1371/journal.pone.0159594.

 doi:10.20944/preprints202601.0045.v1

9. Chen, X.; Stansly, P.A. Biology of Tamarixia radiata (Hymenoptera: Eulophidae), parasitoid of the citrus greening disease vector Diaphorina citri (Hemiptera: Psylloidea): A mini review. *Florida Entomologist* **2014**, *97*, 1404–1413. https://doi.org/10.1653/024.097.0415.
10. George, J.; Ammar, E.D.; Hall, D.G.; Shatters, R.G.; Lapointe, S.L. Prolonged phloem ingestion by Diaphorina citri nymphs compared to adults is correlated with increased acquisition of citrus greening pathogen. *Scientific Reports* **2018**, *8*. https://doi.org/10.1038/s41598-018-28442-6.
11. Camilo, G.G.C. Fluctuación poblacional y tabla de vida Diaphorina citri Kuwayama (Hemiptera: Liviidae) en cultivares de cítricos en las condiciones del municipio de Zona Bananera, Magdalena, 2022.
12. Parra-Fuentes, M.; Pérez-Artiles, L.; Arias-Castro, J.H.; Martínez-Romero, H. Estimation of the reproductive and population parameters of Diaphorina citri (Hemiptera: Liviidae). *Revista Ciência Agronômica* **2025**, *56*, 1–15. https://doi.org/10.5935/1806-6690.20250056.
13. García, Y.; Ramos, P.Y.; Sotelo, P.A.; Kondo, T. Biología de Diaphorina citri (Hemiptera: Liviidae) bajo condiciones de invernadero en Palmira, Colombia. *Revista Colombiana de Entomología* **2016**, *42*, 36–42. https://doi.org/10.XXXX/XXXXXX.
14. Quilici, S.; Joulain, H.; Manikom, R. Étude de la fécondité de Tamarixia radiata (Waterston, 1922) (Hymenoptera: Eulophidae), ectoparasitoïde primaire du psylle asiatique Kuwayama (Homoptera: Psyllidae), vecteur du greening des agrumes. *Fruits* **1992**, *47*, 184–194.
15. Riaño, N.M.; Martínez, M.F.; Orduz-Rodríguez, J.O.; Ríos-Rojas, L.; Galé, Y.L.; Hernández, M.J.Y.; Muñoz, A.C.; Kondo, T.; Muñoz, M.C.G.; González, J.L.; et al. *Modelo productivo de lima ácida Tahití (Citrus × latifolia Tanaka ex Q. Jiménez) para Colombia*; Agrosavia, 2020. https://doi.org/10.21930/agrosavia.model.7403435.
16. Halbert, S.E.; Manjunath, K.L. Asian citrus Psyllids (Sternorrhyncha: Psyllidae) and greening disease of citrus: a literature review and assesment of risk in Florida. *Florida Entomologist* **2004**, *87*, 330 – 353. https://doi.org/10.1653/0015-4040(2004)087[0330:ACPSPA]2.0.CO;2.
17. Gmez-Torres, M.L.; Nava, D.E.; Parra, J.R.P. Life table of tamarixia radiata (Hymenoptera: Eulophidae) on diaphorina citri (Hemiptera: Psyllidae) at different temperatures. *Journal of Economic Entomology* **2012**, *105*, 338–343. https://doi.org/10.1603/EC11280.
18. Martini, X.; Willett, D.S.; Kuhns, E.H.; Stelinski, L.L. Disruption of Vector Host Preference with Plant Volatiles May Reduce Spread of Insect-Transmitted Plant Pathogens. *Journal of Chemical Ecology* **2016**, *42*, 357–367. https://doi.org/10.1007/s10886-016-0695-x.